

# Synthesis, Characterization and Gas Sensing Performance of $\text{PbMnO}_3$ , $\text{PbMnO}_3$ : $\text{SiO}_2$ and $\text{PbMnO}_3$ : $\text{Al}_2\text{O}_3$

A. V. Borhade, \*S. L. Sangle, D. R. Tope

Research Centre, Department of Chemistry, H.P.T. Arts and R.Y.K. Science College, Nasik, Maharashtra, India

## ABSTRACT

The present study reports ecofriendly mechanochemical synthesis of  $\text{PbMnO}_3$ ,  $\text{PbMnO}_3:\text{SiO}_2$  and  $\text{PbMnO}_3:\text{Al}_2\text{O}_3$  composite metal oxides for the first time. The polycrystalline product obtained was analyzed by various physical investigative techniques including FTIR, XRD, SEM, TEM and BET surface area. Screen printed thick films of  $\text{PbMnO}_3$  and modified  $\text{PbMnO}_3$  oxides were prepared to check the potential application for gas sensing properties for most toxic, combustible and hazardous gases  $\text{CO}$ ,  $\text{CO}_2$ ,  $\text{H}_2$ ,  $\text{Cl}_2$ ,  $\text{NH}_3$  and  $\text{H}_2\text{S}$  at different operating temperatures ranging from  $50^\circ\text{C}$  to  $400^\circ\text{C}$ . Among the synthesized sensor  $\text{PbMnO}_3:\text{SiO}_2$  shows highest sensitivity (1740) towards  $\text{NH}_3$  at  $50^\circ\text{C}$  as compared to  $\text{PbMnO}_3$  (71.42) to  $\text{NH}_3$  at  $200^\circ\text{C}$  and  $\text{PbMnO}_3:\text{Al}_2\text{O}_3$  (315.8) to  $\text{H}_2\text{S}$  at  $250^\circ\text{C}$ . This study signifies that sensor was observed to be highly sensitive and selective to  $\text{NH}_3$  and  $\text{H}_2\text{S}$  gas.

**Keywords :**  $\text{PbMnO}_3$ , XRD; BET, Thick Films, Gas Sensing

## I. INTRODUCTION

In recent years, there has been interest in perovskite type of metal oxides containing manganese. These materials show interesting magnetic and electric properties, such as magneto resistivity, nanoscale charge ordering and high oxygen ion conductivity, opening the way to potential applications [1–3]. Gas detection problem was overcome by modified metal oxide semiconducting material. Due to the different applications and inherent limitations of different gas sensing technologies, researchers have been working on different scenarios with enhanced gas sensor calibration. Since 1962 it has been known that absorption or desorption of a gas on the surface of a metal oxide changes the conductivity of the material, so it brings high value of nanocrystalline thick film technology. This phenomenon being first time reported by Sieyama et.al. [1] for zinc oxide thick film.

The response of semiconductor-based sensors is due

to the equilibration of oxygen in the gas phase with ionic and electronic point defects in the oxide semiconductor. The metal oxide most generally used in such sensors is  $\text{SnO}_2$ , but some other oxides like  $\text{TiO}_2$  and  $\text{WO}_3$ , are also used. The perovskite structure obtained from a wide variety of oxides with predominantly ionic conduction transport properties to predominantly electronic conduction. Due to high melting property perovskite, they possess microstructural and morphological stability which is important characteristics to be a long term sensor. Apart from this property, the perovskite structure has two differently-sized cations, which makes possible addition of dopant to it. This doping flexibility is useful for control of the transport and catalytic properties so as to optimize sensor performance for particular applications.

In the market non-dispersive infrared absorption (ND-IR)  $\text{CO}_2$  gas sensors available which are bulky and have high cost [12, 13]. Metal oxides and

modified metal oxides have always been the choice for CO<sub>2</sub> sensor materials [14-18]. Ammonia (NH<sub>3</sub>) and H<sub>2</sub>S is a toxic gas with threshold limit value of 25 ppm for long term exposure (8 h) which are detected by semiconductor metal oxides including SnO<sub>2</sub>, WO<sub>3</sub> and RuO<sub>2</sub> doped ZnO have been reported for detection of NH<sub>3</sub> [19,20]. The operation of these sensors is based on the reversible change of electrical conductance (resistance) which show rise in power consumption reduces sensor life and complicates the design of the sensor [21]. Hence there is need to develop and introduce gas sensor for detecting ammonia (NH<sub>3</sub>) and H<sub>2</sub>S gas for environmental monitoring in chemical industries and research laboratories. Investigation for new and excellent sensor material with their new properties of ordinary material has becomes an important area for research. The doping and coating of metal ion increases the surface area of metal oxide semiconductors which increases the surface area of gas sensor. Hence keeping this view in mind in the present study first time we report on the synthesis of nanocrystalline Lead manganate oxide (PbMnO<sub>3</sub>) by mechanochemical method, SiO<sub>2</sub> composite and Al<sub>2</sub>O<sub>3</sub> composite with PbMnO<sub>3</sub> by hydrothermal method and report as semiconductor-based gas sensors. Various gases like NH<sub>3</sub>, CO<sub>2</sub>, Cl<sub>2</sub>, H<sub>2</sub>S, CO and H<sub>2</sub> at different operating temperature by keeping fixed gas concentration and finally selectivity of different tested gases is compared with each other using these metal oxides. This sensor was observed to be highly sensitive and selective to NH<sub>3</sub> and H<sub>2</sub>S gas. Further the synthesized nanostructure powders were characterized by XRD, SEM, TEM and BET surface area.

## II. EXPERIMENTAL

### 2.1 Materials and Reagents:

Reagents used in this study were purchased and used without further purification: Lead oxide (PbO), Sigma-Aldrich, 99.99 %), Manganese oxide (MnO<sub>2</sub>, Sigma-Aldrich, 99.90 %), sodium hydroxide (NaOH, Merck, 99 %). All gases required were prepared in

laboratory by various chemical reactions.

### 2.2 Synthesis of PbMnO<sub>3</sub>:

Synthesis of perovskite was performed by various techniques which include co-precipitation [17], sol-gel method [18] and thin film vapour deposition method [19]. These methods are laborious, expensive and cause water pollution. In this study, we have synthesized PbMnO<sub>3</sub> by green chemistry approach with mechanochemical process. The mechanochemical procedures are environmentally friendly. The method allows accelerating and facilitating the synthesis processes producing negligible gas emission. It is fast and ecologically pure. In this method, equimolar mixture of Analytical Grade PbO and MnO<sub>2</sub> was grinded with mortar and pestle to attain fine powder for 20 min and heated at 500 °C for 3 h. Again the obtained powder was further heated at 800 °C following milling after each interval of three-hour time. The rise in temperature of muffle furnace was programmed at the rate 10 °C/min from one temperature to the temperature for 12 h. After heating at 500 °C the material was cooled and grounded with gap of 1 h using mortar and pestle. Later on, the ground material was further heated at 800 °C for another 12 h. Finally, polycrystalline powder of PbMnO<sub>3</sub> obtained was used for further characterization preparation of composite metal oxides and for gas sensing performance.

### 2.3 Synthesis of composite PbMnO<sub>3</sub>:SiO<sub>2</sub>:

The PbMnO<sub>3</sub>:SiO<sub>2</sub> sensor was prepared by mixing definite amount of SiO<sub>2</sub> solution (1 mol %) with synthesized PbMnO<sub>3</sub> powder (1 mol %) along with buffer solution. The slurry obtained was stirred for 1 h and transferred into steel lined Teflon autoclave and kept in the oven at 120 °C for 24 h. The precipitate obtained was filtered washed with distilled water and dried at 100 °C for 12 h. The brown polycrystalline product was directly placed in the furnace for calcination at 300 °C for 4 h.

### 2.4 Preparation of composite PbMnO<sub>3</sub>:Al<sub>2</sub>O<sub>3</sub>:

The  $\text{PbMnO}_3:\text{Al}_2\text{O}_3$  sensor was prepared by mixing equimolar amount of  $\text{Al}_2\text{O}_3$  solution (1 mol %) with synthesized  $\text{PbMnO}_3$  powder (1 mol %) along with buffer solution. The slurry obtained was stirred for 15 min. and after stirring this solution was transferred into steel lined Teflon autoclave and kept in the oven for 24 h at  $100^\circ\text{C}$ . Finally the obtained product  $\text{PbMnO}_3:\text{Al}_2\text{O}_3$  was filtered washed with demonized water and dried at  $100^\circ\text{C}$  for 24 h in the oven. The obtained polycrystalline product was heated at  $400^\circ\text{C}$  for 3 h. The obtained products  $\text{PbMnO}_3$ ,  $\text{PbMnO}_3:\text{SiO}_2$  and  $\text{PbMnO}_3:\text{Al}_2\text{O}_3$  were checked for its potential application as a gas sensor.

### 2.5 Characterization:

The XRD profile was obtained recorded on a multipurpose X-ray diffractometer (Philips-1710 diffractometer with  $\text{CuK}\alpha$ ,  $\lambda = 1.5406 \text{ \AA}$ ) at a scan rate of  $0.17^\circ 2\theta \text{ S}^{-1}$ . The scanning electron microscope (SEM) electron micrograph images were taken on a Hitachi SU 70 FESEM with a Schottky electron gun. The Structure and particle size of the synthesized materials were carried out using TEM with SAED on CM-200, Phillips microscope. Quantachrome Autosorb Automated Gas Sorption System Autosorb-1, NOVA-1200 and Mercury Porosimeter Autosorb-1c was used to obtain BET surface area.

### 2.6 Thick film preparation and gas sensing measurements:

The uniform thick paste of synthesized gas sensing materials  $\text{PbMnO}_3$  and its composite was prepared by thoroughly mixing its fine powder with 30 wt % organic binder (ethyl cellulose), 30 wt % solvent (2-butoxyethanol and terpineol) and 15 ml dispersant. The films were prepared on glass substrate by using screen printing followed by drying under tungsten filament lamp. Dried films were fired at  $450^\circ\text{C}$  for 1 h for the complete removal of organic binder. The gas sensing property of three sensors have been studied using static gas sensing system towards various gases. The current developed was measured by a digital Picoammeter by applying constant voltage to the

sensor. The current passing through the heating element was monitored using with an electronic circuit with adjustable on-off time intervals. A Cr-Al thermocouple was used to sense the operating temperature of the sensor. The output of the thermocouple was connected to a digital temperature indicator. The heater was fixed on the base plate to heat the sample up to required operating temperatures. A gas inlet valve was fitted to the base plate, the required gas concentration inside the static system was achieved by injecting a known volume of a gas using gas injecting syringe. The air was allowed to pass into the glass chamber after every gas exposure cycle. The complete illustration of gas sensing apparatus is shown in Fig. 1.

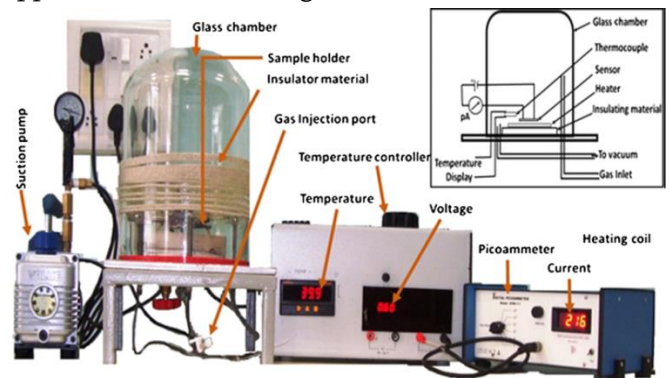


Fig 1. Steady gas sensing system photograph with block diagram

Finally the sensitivity of thick films were checked for  $\text{NH}_3$ ,  $\text{H}_2\text{S}$ ,  $\text{H}_2$ ,  $\text{CO}_2$ ,  $\text{CO}$  and  $\text{Cl}_2$  gases for the temperature range of  $50^\circ\text{C}$  to  $400^\circ\text{C}$  with various gas concentration (50-100 ppm). The changes in resistance on contact between target gas and sensor were measured from steady gas sensing system. The ratio of change in conductance of sample on exposure to a test gas ( $G_{\text{gas}}$ ) to the conductance in air ( $G_{\text{air}}$ ) is known as sensitivity and is simply defined as,

$$\text{Sensitivity} = \frac{G_{\text{gas}} - G_{\text{air}}}{G_{\text{air}}}$$

Where  $R_a$  is the resistance of metal oxide film in the presence of dry air and  $R_g$  the resistance of metal oxide film in presence of test gas.

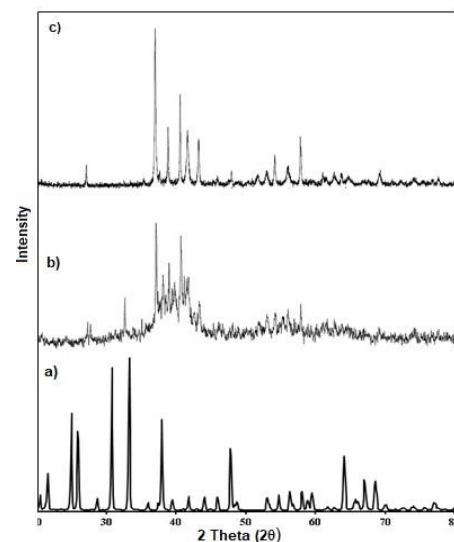
### III. Results and Discussion

#### 3.1 General:

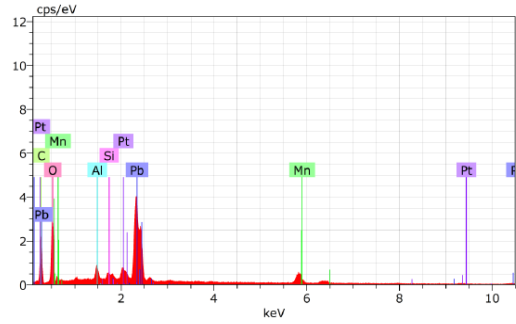
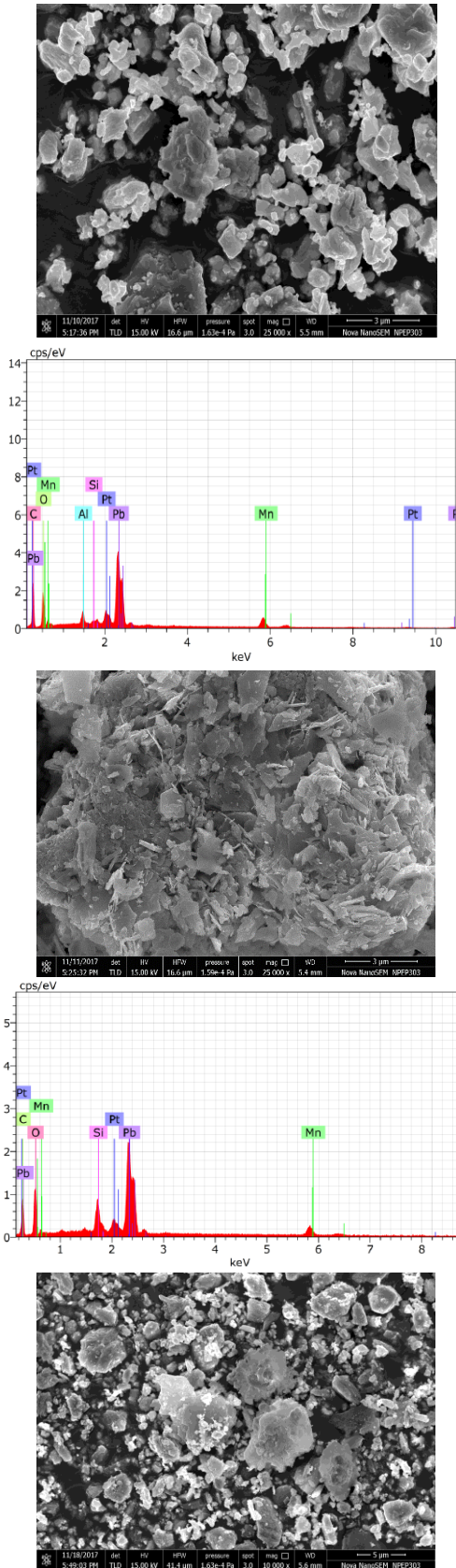
Hydrothermally synthesized products ( $\text{PbMnO}_3:\text{SiO}_2$  and  $\text{PbMnO}_3:\text{Al}_2\text{O}_3$ ) were calcined at  $600^\circ\text{C}$  for 3 h to remove organic matter and then analyzed by X-ray diffraction method. XRD pattern obtained for all three product shows that they are polycrystalline in nature. The XRD pattern recorded for pure  $\text{PbMnO}_3$  (Fig. 2a) shows  $2\theta$  values along with (hkl) planes at  $26.34$  (110),  $29.06$  (100),  $30.5$  (100),  $32$  (110),  $50.74$  (200). These peaks in the XRD profile well matches with JCPDS data (Card No. 254301) and confirm the crystals are cubic in nature. Figure 2b gives XRD pattern for  $\text{PbMnO}_3:\text{SiO}_2$ . The  $2\theta$  values in connection with (hkl) plane are  $26.4$  (100),  $26.52$  (110),  $28.72$  (222),  $38.4$  (102),  $44.4$  (110),  $52.3$  (200)  $59.3$  (220). The recorded XRD pattern shows there is no any amorphous phase found and it reveals that product is highly polycrystalline with cubic in nature. The XRD analysis of  $\text{PbMnO}_3:\text{Al}_2\text{O}_3$  shows sharp peaks at  $33.96$  (100),  $34$  (200),  $38.5$  (100),  $47.46$  (110),  $52.4$  (101) and extra peaks due to Al coating at  $2\theta$  values  $25.7$ ,  $37.8$ ,  $40.8$  and  $51.9$  (Fig. 2c). All these obtained peaks are well relevant to JCPDS card number data confirming with cubic structure.

The SEM analysis of  $\text{PbMnO}_3$  and  $\text{PbMnO}_3:\text{Al}_2\text{O}_3$  shoes agglomeration whereas  $\text{PbMnO}_3:\text{SiO}_2$  gives rod like morphology. The EDAX analysis confirms the formation of  $\text{PbMnO}_3$ ,  $\text{PbMnO}_3:\text{SiO}_2$  and  $\text{PbMnO}_3:\text{Al}_2\text{O}_3$  with appropriate stoichiometry. SEM images along with EDAX analysis obtained for synthesized three nanocrystalline products are shown in Fig. 3a-c. TEM images along with SAED pattern obtained for synthesized three nanocrystalline products are shown in Fig. 4a-c. From Fig. 4a one can observe that most of the  $\text{PbMnO}_3$  crystals are cubic in nature. The particle size obtained by TEM for  $\text{PbMnO}_3$  is found to be  $187$  nm. The particle size for  $\text{PbMnO}_3:\text{SiO}_2$  by TEM is  $32.27$  nm (Fig.4b). TEM

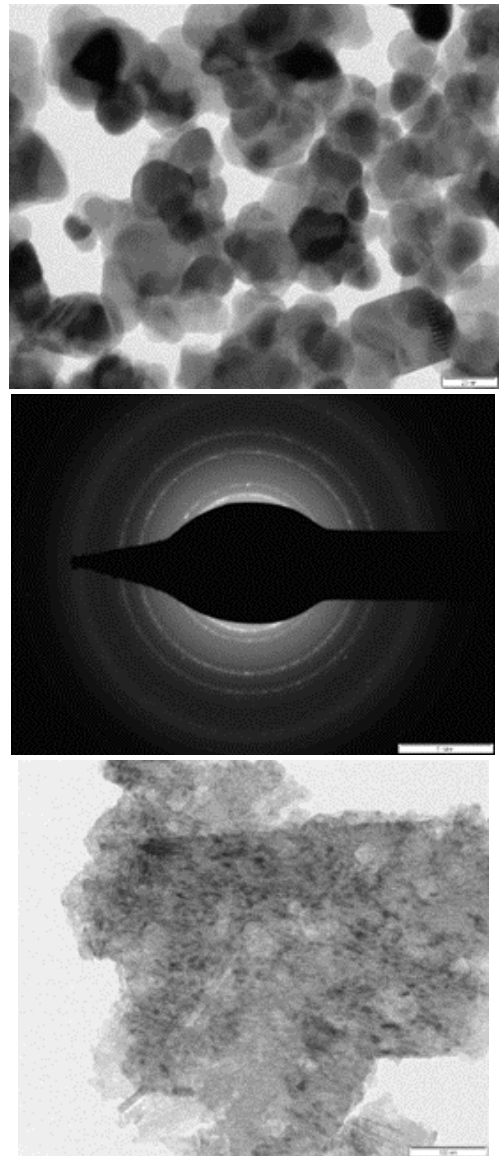
analysis clearly reveals that crystals are cubic in nature and it well matches with XRD analysis. The particle size obtained for  $\text{PbMnO}_3:\text{Al}_2\text{O}_3$  is  $53.89$  nm (Fig.4c). This figure shows that some of the crystals are big and hexagonal and most of them are cubic in nature. Surface area of material plays an important role in catalysis and gas sensing properties. In the present the typical  $\text{N}_2$  adsorption/desorption isotherm and BJH pore distribution of prepared  $\text{PbMnO}_3$ ,  $\text{PbMnO}_3:\text{SiO}_2$  and  $\text{PbMnO}_3:\text{Al}_2\text{O}_3$  are nearly same in curve shape which are depicted in Fig. 5a-c. This method (BET) leads to the identification of the isotherm profile as type IV in the BDDT system which is typical for mesoporous material. The BJH pore size distribution demonstrates that all the samples obtained have narrow pore diameter range. The BET surface area ( $S_{\text{BET}}$ ), pore volume ( $V_p$ ), pore diameter ( $D_p$ ) and other parameters are recorded in Table 1. This clearly gives evidence that the doping and coating of metal ions with  $\text{PbMnO}_3$  shows increase in large surface area (Table 1). A careful inspection of Table 1 shows that the surface area was found to be highest for  $\text{PbMnO}_3$  is  $187.9$   $\text{cm}^2/\text{g}$ , the average pore volume ( $V_p$ ) and pore diameter ( $D_p$ ) were  $0.0657$   $\text{cc/g}$  and  $18.88$   $\text{\AA}$  respectively. For  $\text{PbMnO}_3:\text{SiO}_2$   $179.26$   $\text{cm}^2/\text{g}$ , the average pore volume ( $V_p$ ) and pore diameter ( $D_p$ ) were  $0.0317$   $\text{cc/g}$  and  $37.76$   $\text{\AA}$  respectively. For  $\text{PbMnO}_3:\text{Al}_2\text{O}_3$  the BET surface area is  $97.67$   $\text{cm}^2/\text{g}$ , the average pore volume ( $V_p$ ) and pore diameter ( $D_p$ ) were  $0.0317$   $\text{cc/g}$  and  $65.10$   $\text{\AA}$  respectively.



**Fig.2:** XRD analysis of (a)  $\text{PbMnO}_3$ , (b)  $\text{PbMnO}_3:\text{SiO}_2$  and (c)  $\text{PbMnO}_3:\text{Al}_2\text{O}_3$



**Fig. 3:** SEM and EDAX analysis of a)  $\text{PbMnO}_3$ , b)  $\text{PbMnO}_3:\text{SiO}_2$  and c)  $\text{PbMnO}_3:\text{Al}_2\text{O}_3$ .



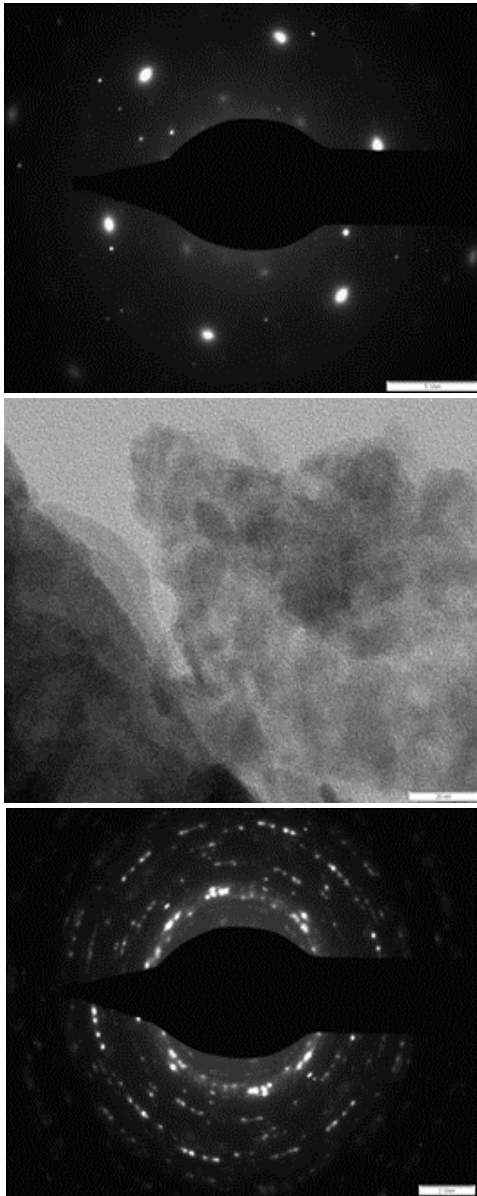


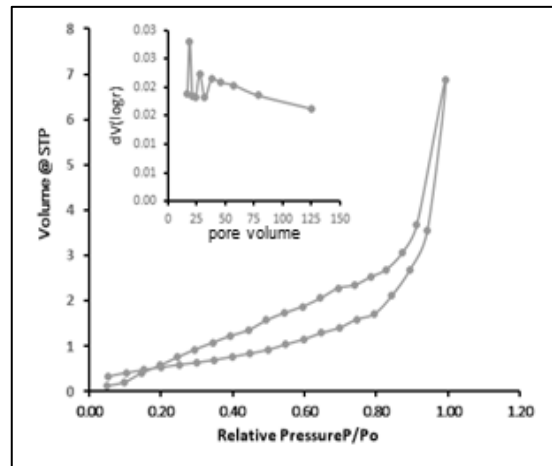
Fig. 4: TEM and SAED pattern of a)  $PbMnO_3$ , b)  $PbMnO_3:SiO_2$  and c)  $PbMnO_3:Al_2O_3$ .

Table 1 : BET surface area, pore volume and pore diameter of  $PbMnO_3$ ,  $PbMnO_3:SiO_2$  and  $PbMnO_3:Al_2O_3$

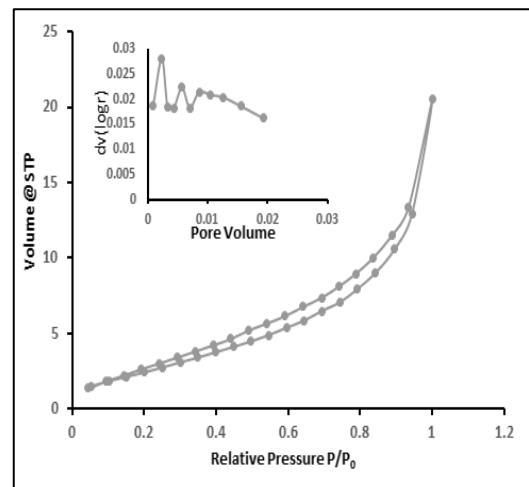
Synthesized compound	Surface area ( $m^2/g$ )	Pore volume ( $cc/g$ )	Pore diameter ( $\text{\AA}$ )
$PbMnO_3$	187.9	0.0106	18.88
$PbMnO_3:SiO_2$	179.26	0.0317	65.10
$PbMnO_3:Al_2O_3$	97.67	0.0657	37.76

### 3.2 Selectivity of $PbMnO_3$ , $PbMnO_3:SiO_2$ and $PbMnO_3:Al_2O_3$ thick films for various gases:

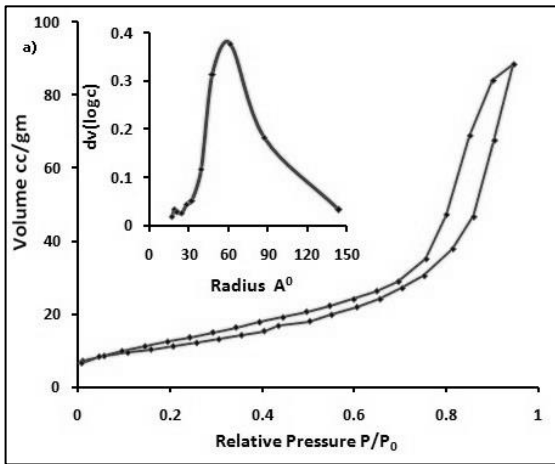
Figure 5a-c depicts selectivity of sensing materials  $PbMnO_3$  and modified  $PbMnO_3$  towards various gases  $NH_3$ ,  $H_2S$ ,  $H_2$ ,  $CO_2$ ,  $CO$  and  $Cl_2$ . Figure 5a-c also shows the operating temperature change from  $50\text{ }^\circ C$  to  $400\text{ }^\circ C$  with 500 ppm of each gas. The results obtained reveals that the  $PbMnO_3$  thick film gives maximum sensitivity to  $NH_3$  (71.42) at temperature  $200\text{ }^\circ C$ . Further  $PbMnO_3:Al_2O_3$  gives highest sensitivity to  $H_2S$  (315.8) at  $250\text{ }^\circ C$  But  $PbMnO_3:SiO_2$  clearly shows this thick film act as a  $NH_3$  gas sensor with highest sensitivity 1740 at temperature  $50\text{ }^\circ C$  as compared to  $PbMnO_3:Al_2O_3$  and  $PbMnO_3$  (Fig. 5c). This study clearly reveals that as the  $PbMnO_3$  modified it response to different gases.



(a)



(b)



(c)

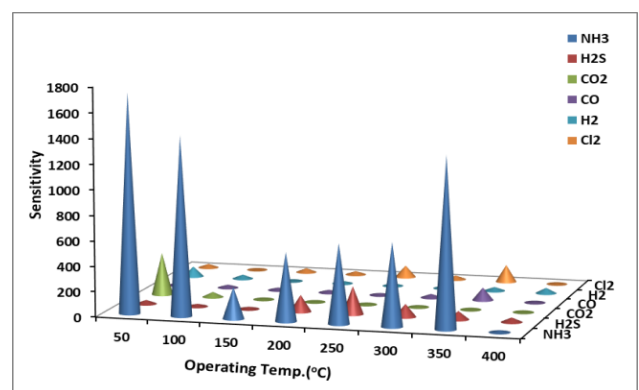
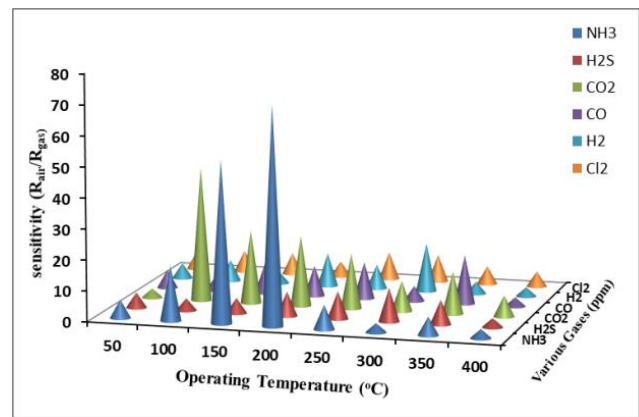
Fig. 5 : BET analysis of (a) PbMnO<sub>3</sub>, (b) PbMnO<sub>3</sub>:SiO<sub>2</sub> and (c) PbMnO<sub>3</sub>:Al<sub>2</sub>O<sub>3</sub>.

### 3.3 Selectivity of PbMnO<sub>3</sub>, PbMnO<sub>3</sub>: SiO<sub>2</sub> and PbMnO<sub>3</sub>: Al<sub>2</sub>O<sub>3</sub> for NH<sub>3</sub> and H<sub>2</sub>S gas with various operating temperature:

A particular sensing material shows highest gas response for a particular gas at a particular temperature. Using this method specific gas may be sensed by setting the temperature. Various gases show different energies for adsorption reaction on the metal oxide surface and hence response at various temperature depends on the gas being sensed. In the present investigation effect of annealing temperature 250 °C-450 °C on the sensitivity of PbMnO<sub>3</sub>, PbMnO<sub>3</sub>:SiO<sub>2</sub> and PbMnO<sub>3</sub>:Al<sub>2</sub>O<sub>3</sub> on 500 ppm of NH<sub>3</sub> and H<sub>2</sub>S are carried out (Fig. 6a-c). For the sake of comparison NH<sub>3</sub> gas sensing property of PbMnO<sub>3</sub>, PbMnO<sub>3</sub>: SiO<sub>2</sub> and H<sub>2</sub>S for PbMnO<sub>3</sub>: Al<sub>2</sub>O<sub>3</sub> thick films at different temperatures were also studied under identical annealing condition of temperature. Fabrication of sensors for gas sensing material is mainly depending upon annealing temperature. The sensing material must be annealed at various temperatures to obtain crystallization and structure determination. Because degree of crystallinity is important to attain the desired electronic properties which are prime importance for gas sensor application. In the present study the dependence of sensitivity of the synthesized PbMnO<sub>3</sub> at 500 ppm for NH<sub>3</sub>, PbMnO<sub>3</sub>:Al<sub>2</sub>O<sub>3</sub> for H<sub>2</sub>S and PbMnO<sub>3</sub>:SiO<sub>2</sub> for NH<sub>3</sub> at

annealing temperature of 250, 300, 350, 400 and 450 °C along with the operating temperature is visualized.

It was observed that the annealing in air renders more oxygen vacancy generation which increases H<sub>2</sub>S gas sensing for PbMnO<sub>3</sub>:Al<sub>2</sub>O<sub>3</sub> and NH<sub>3</sub> gas sensing for PbMnO<sub>3</sub> and PbMnO<sub>3</sub>:SiO<sub>2</sub>. Further the keen observation of Fig. 6a-c shows that the sensitivity increases from 50 °C to 200 °C and later it decreases with further increase in the operating temperature. The maximum sensitivity was found to NH<sub>3</sub> gas for PbMnO<sub>3</sub>:SiO<sub>2</sub> thick film is 1740, PbMnO<sub>3</sub> thick film shows 71.42 to NH<sub>3</sub> gas and PbMnO<sub>3</sub>:Al<sub>2</sub>O<sub>3</sub> shows 315.8 for H<sub>2</sub>S at annealing temperature 50 °C, 200 and 250 °C for 500 ppm each gas respectively.



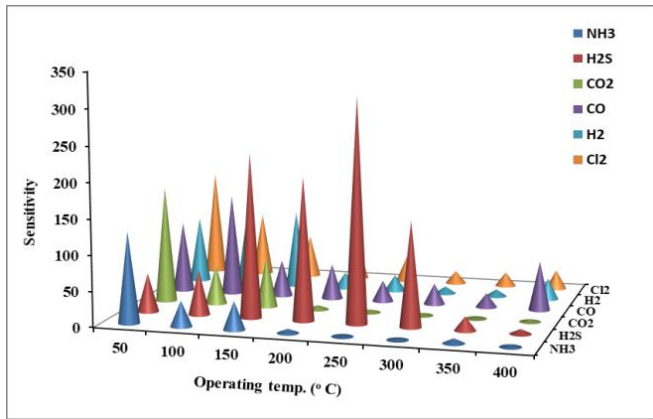


**Fig. 6.** Sensitivity of various gases at various temperatures on gas response for (a) PbMnO<sub>3</sub>, (b) PbMnO<sub>3</sub>:SiO<sub>2</sub> and (c) PbMnO<sub>3</sub>:Al<sub>2</sub>O<sub>3</sub>.

### 3.4 Variation in sensitivity with gas concentration:

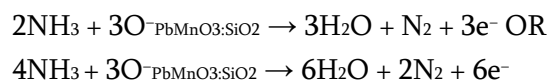
The dependence of sensitivity of PbMnO<sub>3</sub>, PbMnO<sub>3</sub>:SiO<sub>2</sub> and PbMnO<sub>3</sub>:Al<sub>2</sub>O<sub>3</sub> on the NH<sub>3</sub> and H<sub>2</sub>S gas concentration at an operating temperature 50°C and is presented in Fig. 7a–c. It is observed that the sensitivity increases substantially in all three sensors prepared. In case of these three catalysts the gas concentration varied from 200 to 1000 ppm and then decreases with further increase in all three gas concentration. This linearity between gas concentration and sensitivity with lower concentration may be attributed to the availability of sufficient number of sensing sites on the film to act upon NH<sub>3</sub>. Lowering in concentration shows that the surface coverage of gas molecules and hence less surface reaction between the surfaces adsorbed oxygen species and the gas molecules. With increase in the gas concentration increases the surface reaction due to a large surface coverage. In the present study the maximum sensitivity was obtained at an operating temperature 50 °C for the exposure of 1000 ppm of NH<sub>3</sub> gas.

The obtained linearity of thick film sensitivity in the low NH<sub>3</sub> concentration range (200-1000 ppm) suggests that the PbMnO<sub>3</sub>, PbMnO<sub>3</sub>:SiO<sub>2</sub> and PbMnO<sub>3</sub>:Al<sub>2</sub>O<sub>3</sub> can be properly applied to monitor the concentration of NH<sub>3</sub> over the range studied.

### 3.5 Sensitivity mechanism of PbMnO<sub>3</sub>:SiO<sub>2</sub> thick film as NH<sub>3</sub> gas sensor:

The surface of PbMnO<sub>3</sub>:SiO<sub>2</sub> adsorbs atmospheric oxygen molecule in the form of O<sup>-</sup> or O<sup>2-</sup> and hence conductivity decreases. These oxygen molecules takes electron from PbMnO<sub>3</sub>:SiO<sub>2</sub> in the form of adsorbed O<sup>-</sup> PbMnO<sub>3</sub>:SiO<sub>2</sub>. The process occurs in the form of O<sub>2(g)</sub> + 2e<sup>-</sup> → 2O<sup>-</sup> PbMnO<sub>3</sub>:SiO<sub>2</sub>

Then PbMnO<sub>3</sub>:SiO<sub>2</sub> becomes oxygen deficient. In the present study when reducing gas NH<sub>3</sub> reacts with negatively charged oxygen adsorbate then the trapped electrons are given back to conduction band of PbMnO<sub>3</sub>:SiO<sub>2</sub>. The adsorbed ammonia gets decomposed releasing some energy ease of this electron jump into the conduction band of PbMnO<sub>3</sub>:SiO<sub>2</sub> giving increase in the conductivity of the sensor. Hence the possible mechanism proposed for PbMnO<sub>3</sub>:SiO<sub>2</sub> towards NH<sub>3</sub> is,



Increase in operating temperature increases the thermal energy causing oxidation of NH<sub>3</sub> and hence NH<sub>3</sub> donates electrons to PbMnO<sub>3</sub>:SiO<sub>2</sub>. This confirms gas response rises with an operating temperature due to decrease in resistance. The maximum values of sensitivity indicate this is the actual energy needed to proceed the reaction. But at very high temperature desorption takes place because oxygen adsorbates are desorbed from the surface of the sensor [22].

### 3.6 Sensitivity mechanism of PbMnO<sub>3</sub> and PbMnO<sub>3</sub>:SiO<sub>2</sub> thick films to NH<sub>3</sub> gas sensor:

The PbMnO<sub>3</sub>:SiO<sub>2</sub> thick film was surface modified by coating SiO<sub>2</sub> particles were distributed homogeneously on the surface of the PbMnO<sub>3</sub>:SiO<sub>2</sub>. The coating of SiO<sub>2</sub> enhance the catalytic reaction efficiently and the overall change in resistance on exposure of reducing gas (NH<sub>3</sub>) leads to rise in



sensitivity. The thick film gas sensing mechanism of  $\text{PbMnO}_3:\text{SiO}_2$  is mainly based on surface modification of material synthesized. The sensing material adsorbs molecular oxygen from air and gets dissociated to various species like  $\text{O}^-$ ,  $\text{O}^{2-}$  and  $\text{O}^{2-}$ . The  $\text{O}^{2-}$ -adsorbed oxygen ions on surface of sensing material and the oxide particles form a depletion layer. This depletion layer creates an electric field between adsorbed oxygen species and the metal oxide species. At definite temperature  $\text{NH}_3$  gas can be oxidized into  $\text{NO}_2^-$  by reacting with adsorbed oxygen. The nitroxide formed diminishes when it is exposed to oxidizing conditions [23]. When gas response is measured during high temperature, the desorption of gas leads to the sensitivity of the material. The sensitivity of these oxygen species mainly depends on the operating temperature [24]. When the thick film of  $\text{PbMnO}_3$  and  $\text{PbMnO}_3:\text{SiO}_2$  was fully exposed to  $\text{NH}_3$  gas then the species  $\text{O}^-$  reacts with  $\text{NH}_3$  gas and extracts the electrons from the conduction band of the n-type  $\text{PbMnO}_3$  thick film. This shows that the amount of number of electrons on the surface of  $\text{PbMnO}_3:\text{SiO}_2$  decreases and hence the film resistance as found to be increase.

### 3.7 Gas Response and Recovery

The response and recovery time for the most sensitive  $\text{PbMnO}_3:\text{SiO}_2$  during a week are represented in Fig. 7. The gas response for  $\text{NH}_3$  with concentration 100 ppm at  $50^\circ\text{C}$  was quick (4 s) and recovery time was 22 s. These results showed that the sensors have an excellent stability towards the  $\text{NH}_3$  gas. There is no baseline shifting. The gas sensing response and recovery times are important parameters to evaluate the performance of a gas sensor.

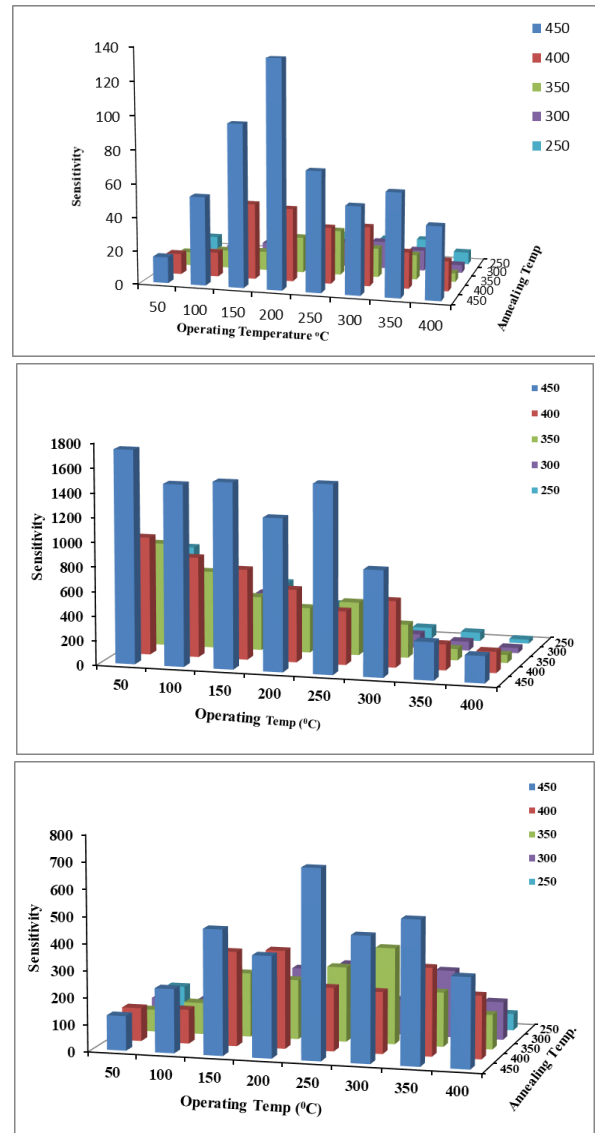


Fig. 7. Effect of annealing temperatures operating for a)  $\text{PbMnO}_3$  for  $\text{NH}_3$  gas, b)  $\text{PbMnO}_3:\text{SiO}_2$  for  $\text{NH}_3$  gas and c)  $\text{PbMnO}_3:\text{Al}_2\text{O}_3$  for  $\text{H}_2\text{S}$  gas

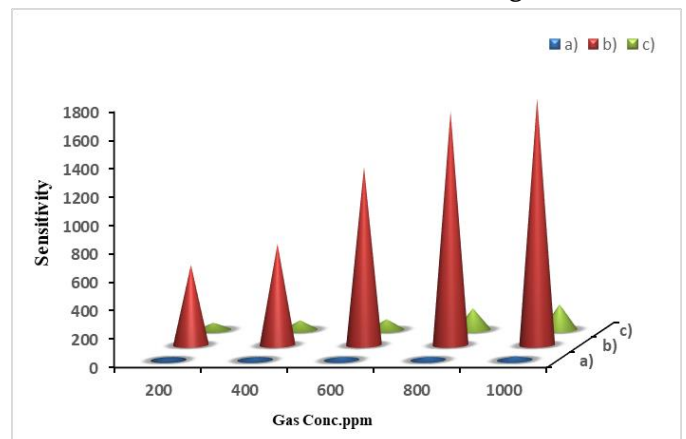
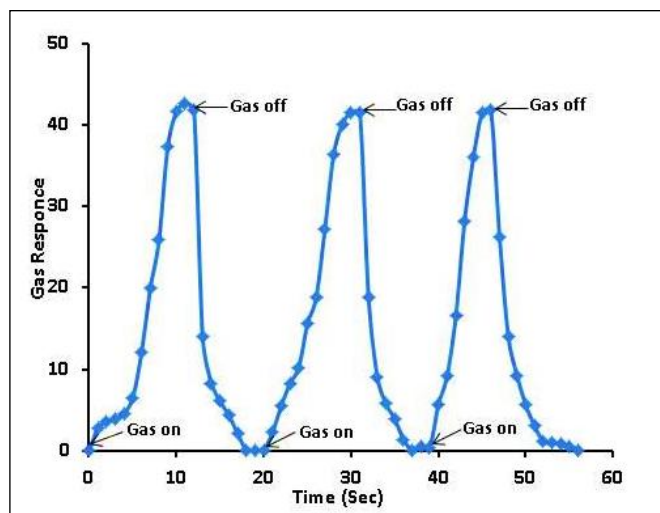


Fig. 8. Effect of  $\text{NH}_3$  gas concentration on sensitivity (a)  $\text{PbMnO}_3$ , (b)  $\text{PbMnO}_3:\text{SiO}_2$  and (c)  $\text{PbMnO}_3:\text{Al}_2\text{O}_3$



**Fig. 9:** Gas response and gas recovery of  $\text{NH}_3$  gas with  $\text{PbMnO}_3:\text{SiO}_2$  catalyst.

#### IV. CONCLUSION

Nanocrystalline  $\text{PbMnO}_3$  and modified  $\text{PbMnO}_3$  are successfully prepared by mechanochemical and hydrothermal method. The thick film for these materials was prepared by screen printing method. The prepared thick films were applied for sensing of different gases. Following important conclusions were drawn from the present study

1. The unmodified  $\text{PbMnO}_3$  thick film was found to be  $\text{NH}_3$  sensitive at  $200^\circ\text{C}$ .
2.  $\text{PbMnO}_3:\text{SiO}_2$  sensor is selective to  $\text{NH}_3$  gas and forbidden the response to other gases.
3.  $\text{PbMnO}_3:\text{Al}_2\text{O}_3$  sensor is found to be highly sensitive to  $\text{H}_2\text{S}$  gas.
4. Gas sensing mechanism for each gas with sensing material was established successfully.
5. Modification of  $\text{PbMnO}_3$  alters the gas sensing properties.

#### V. REFERENCES

- [1]. KA. Seiyama, K. Fujiishi, M. Nagarani, *Anal. Chem.* 34, 1502 (1962)
- [2]. N Yamazoe, Y. Kurokawa, T. Seiyam, *Sens. Actuators.* 4, 283 (1983)
- [3]. T Kabayashi, M. Haruta, H. Sano, M. Nakane, *Sens. Actuators.* 13, 339 (1988)
- [4]. J Tamaki, T. Maekawa, S. Matsushima, N. Miura, N. Yamazoe, *Chem. Lett.* 19, 477 (1990)
- [5]. U Lampe, J. Gerblinger, H. Meixner, *Sens. Actuators B Chem.* 25, 657 (1995)
- [6]. Y Nakamura, H. Zhang, A. Kishimoto, O. Okada, H. Yanagida, *J. Electrochem. Soc.* 145, 632 (1998)
- [7]. W.H. TaO, C.H. Tsai, *Sens. Actuators B Chem.* 81, 237 (2002)
- [8]. C. Cantalini, *Sens. Actuators B Chem.* 24, 1421 (2004)
- [9]. J.D. Shakun, P.U. Clark, H. Feng, S.A. Marcott, A.C. Mix, L. Zhengyu, B. Bliesner, A. Schmittner, E. Bard, *Nature.* 49, 484 (2002)
- [10]. P. Puligundla, J. Jung, S. Ko, *Food Control* 25, 328 (2012)
- [11]. G. Eranna, B.C. Joshi, D.P. Runthala, R. Gupta, *Crit. Rev. Solid State Mater. Sci.* 29, 111 (2004)
- [12]. T. Yasuda, S. Yonemura, A. Toni, *Sensors* 12, 3641 (2012)
- [13]. B. H. Chu, C. Y. Chang, S. J. Pearton, J. Lin, F. Ren eds., *Chemical and Biomedical Applications* (CRC Press, Boca Ratan, 2011), pp. 47-48
- [14]. N.T.R.N. Samarasekara, P. Kumara, N.U.S. Yapa, *J. Phys. Condens. Matter* 18, 2417 (2006)
- [15]. T. Krishnakumar, R. Jayprakash, T. Prakash, D. Satyaraj, N. Donato, S. Licoccia, M. Latino, A. Stassi, *G. Neri Nanotechnology* 22, 325501 (2011)
- [16]. A. Marsal, A. Cornet, J.R. Morante, *Sens. Actuators B Chem.* 94, 324 (2003)
- [17]. J. Herran, G.G. Mandayo, E. Castano, *Sens. Actuators B Chem.* 129, 705 (2008)
- [18]. C.R. Michel, A.H. Martinez, F.H. Villalpando, J.P.M. Lazaro, *J. Alloys Compd.* 484, 605 (2009)
- [19]. G. Sberreglieri, L. Depero, S. Gropelli, P. Nelli, *Sens. Actuators B Chem.* 89, 26 (1995)
- [20]. M.S. Wagh, G.H. Jain, D.R. Patil, S.A. Patil, L. A. Patil, *Sens. Actuators B Chem.* 20, 55 (1994)
- [21]. C.L. Johnson, J.W. Schwank, K.D. Wise, *Sens. Actuators B Chem.* 20, 55 (1994)
- [22]. H. Windichmann, P. Mark, *J. Electrochem. Soc.* 126, 627 (1979)
- [23]. K. Wetchokun et al., *Sens. Actuators B Chem.* 160, 580-591 (2007)
- [24]. P.E. Caro, J.O. Sowyer, L. Eyring, *Spectra Acta* 28, 1167 (1971)